Semileptonic Vector Boson Scattering at the ATLAS Detector
and
Planar Pixel Sensors for the ATLAS ITk

CAT Student Seminar

Tobias Fitschen

2021-05-10

Why study VBS?

Vector Boson Scattering (VBS) **and** **Vector Boson Fusion (VBF)**

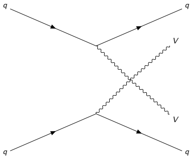

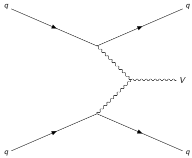

... are sensitive to:

trilinear gauge coupling

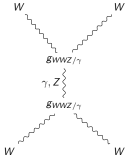

quartic gauge coupling

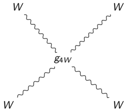

hVV coupling

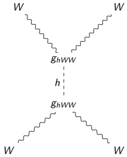

Each diagram individually is divergent towards high energies

But divergences precisely cancel:

→ Highly sensitive probe for electroweak physics

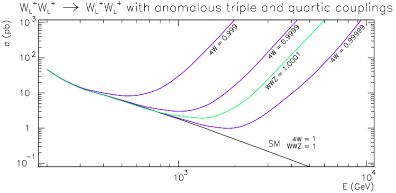

source: arXiv:1412.8367

There is no such thing as a VBS/VBF measurement on its own!

Gauge invariant set of Vjj/ VVjj diagrams at $\mathcal{O}(\alpha_W^3)$ / $\mathcal{O}(\alpha_W^4)$ tree level:

VBF/VBS **Weak Boson Bremsstrahlung**

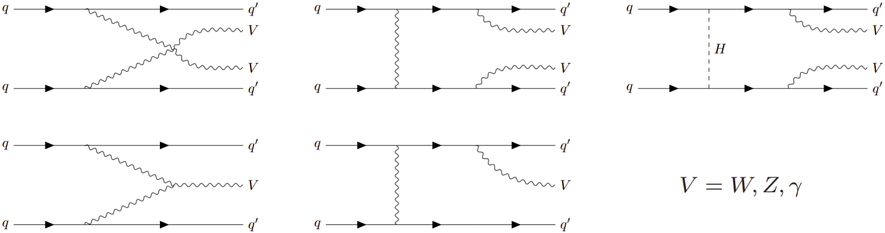

$V = W, Z, \gamma$

- Negative interference between VBS/VBF and weak boson bremsstrahlung
- Instead: measure **electroweak (EW) production of Vjj and VVjj**
- In this presentation: Semileptonic *VVjj*

The ATLAS Detector

Common experimental signature of VBS events:

- Dijet system *jj* with large invariant mass m_{jj}
- Different sides/hemispheres of the detector
- Large angular separation

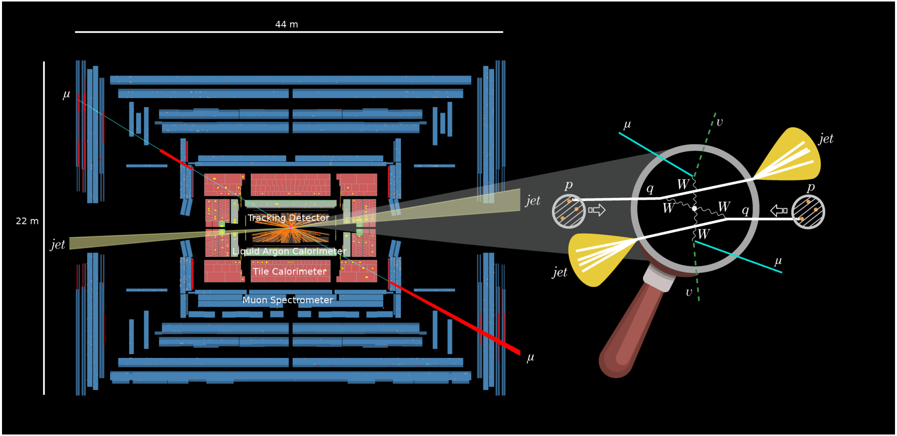

Simplified event display of a fully leptonic VBS candidate event in the ATLAS detector

source: ATLAS-PHOTO-2020-037-4 (modified)

Semileptonic VBS

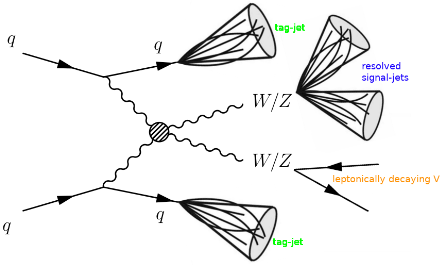

Analysis Goals:

- Measure EW $VVjj$
- Cross-section in fiducial region
  $\rightarrow$ Differential if possible
- EFT interpretation
  $\rightarrow$ Search for aQGC
  $\rightarrow$ Sensitivity in high p_{T} needed

Final State:

- **2 tagging jets**:
  Forward
  Opposite Hemispheres
- **1 boson decays hadronically**:
  2 $R = 0.4$ signal jets (**resolved**)
  or 1 $R = 1.0$ signal jet (**merged**)

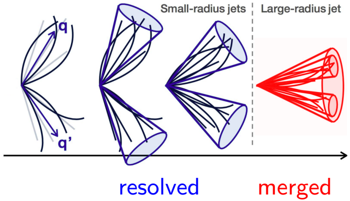

- **1 boson decays leptonically**:
  0-lepton: $Z \rightarrow \nu\nu$
  1-lepton: $W \rightarrow \ell\nu$
  2-lepton: $Z \rightarrow \ell\ell$

Previous Analysis

August 2019: Previous Analysis with 35.5 fb^{-1}: Phys. Rev. D 100, 032007

- Simultaneous max-likelihood fit on BDT outputs in all SRs and CRs
- Cross-section measurement in fiducial region

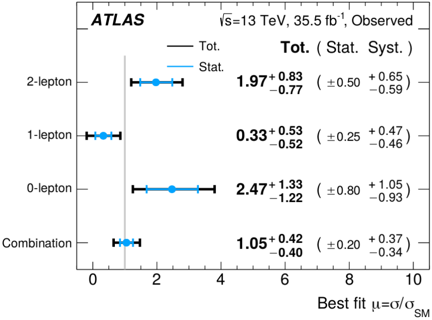

- Signal strength: $\mu^{\text{obs}}_{\text{EWVVjj}} = 1.05 \pm 0.20(\text{stat})^{+0.37}_{-0.34}(\text{syst})$
- Significance: $n^{\text{obs}}_{\sigma} = 2.7$, $n^{\text{exp}}_{\sigma} = 2.5$

source: Phys. Rev. D 100, 032007

0-Lepton Event Selection

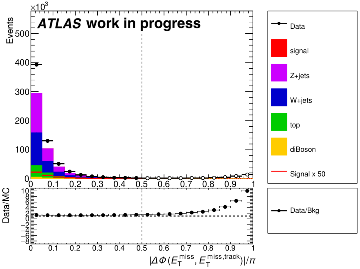

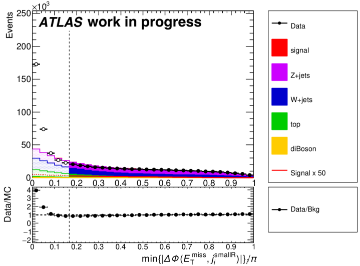

Pileup reduction:

- Pileup affects tracker and calorimeters differently

→ Exclude events with small $E_T^{miss,track}$ magnitude

→ And with $E_T^{miss,track}$ in different direction in Φ than E_T^{miss}

QCD multijet rejection:

- No reliable Monte Carlo for QCD background available
- Must be reduced in data
- QCD events typically only pass E_T^{miss} selection if single mismeasured jet j contributes significantly to E_T^{miss}

→ Small distance $\Delta\Phi$ of j to E_T^{miss}

Two approaches for MVA final discriminant:

- **Baseline:** Full selection (tag jets & signal jets), multi variate analysis on high level variables
- **RNN approach:** Only signal-, no tag-jet selection, rely on recurrent neural network (RNN) with four-vecor input from all jets to distinguish VBS from non-VBS

Signal composition in merged SR

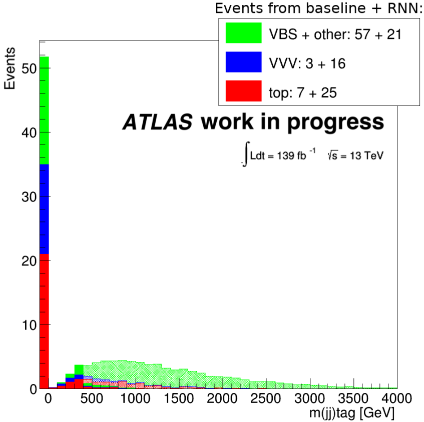

- **Hatched:** Baseline selection
- **Filled:** Additional events from RNN approach (dropping tag-jet selection)
- **Underflow bin:** No two tagging jets reconstructed

Top processes

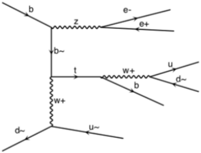

Triboson processes

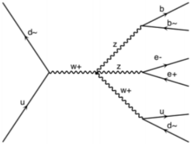

→ Most events added by RNN approach do not have reconstructed tag-jets

Summary & Outlook

Semileptonic Vector Boson Scattering at the ATLAS detector

Summary:

- Previous analysis significance: $n_{\sigma}^{\text{obs}} = 2.7$ at 35.5 fb^{-1}

- **New study with 139 fb^{-1} in progress:**
  - Cross section measurement of semileptonic EWK VVjj in fiducial region
  - aQGC study with EFT approach in progress
  - Studies on signal composition (VBS/ non-VBS contributions)

  - **Two approaches for MVA final discriminant:**
    - **Baseline:** full selection (tag jets & signal jets) and then BDT or NN
    - **RNN approach:** only signal-, no tag jet selection, then RNN
    - Novel RNN approach must be verified against baseline

Goal:

- Obtain 5 sigma observation of the VBS process in semileptonic final state

Part II:

Planar Pixel Sensors for the ATLAS ITk

LHC Upgrade

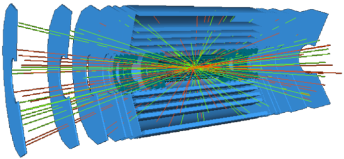

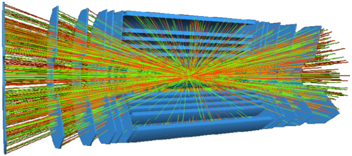

- LHC will be upgraded to High-Luminosity (HL-LHC)
- $\approx 60 \rightarrow 200$ interactions per bunch crossing
- Current inner detector must be upgraded to satisfy new requirements

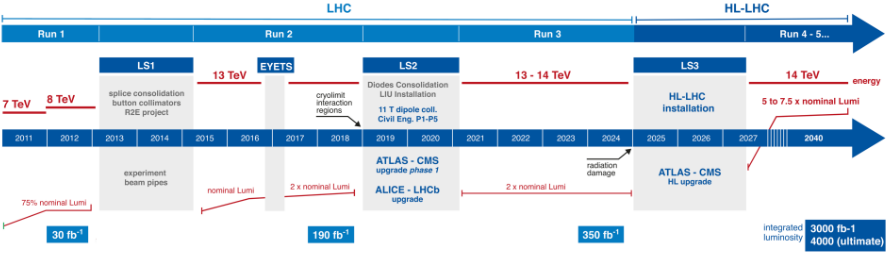

The ITk Detector

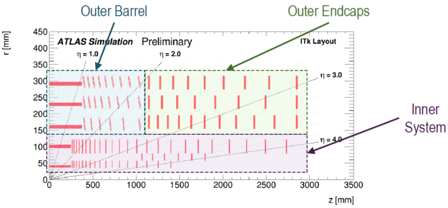

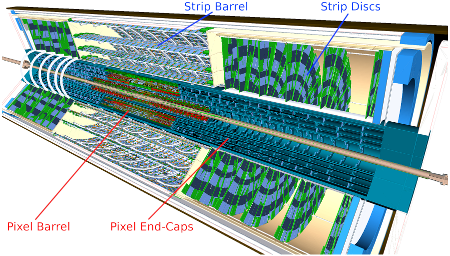

ATLAS ITk Pixel TDR, CERN-LHCC-2017-005

Inner Detector (ID) will be replaced by full-Si Tracker (ITk):

- Has to be able to survive the harsh radiation environment of the HL-LHC
- Increased coverage up to 4 η with at least 9 points per track
- Outer Part: Si-strip detectors:
- Inner Part: 5 layers of **Si-pixel detectors** (covered in this talk):
  - Inner layer (L0): 1188 3D sensors (150 μm), 34 mm from beam
  - Outer layer (L1): 1200 planar sensors (100 μm)
  - Outer barrel and endcap (L2-4): 6816 planar sensors (150 μm)

Current pixel system		**New ITk pixel system**
~1.9 m^2 of active area	➤	~13 m^2 of active area
2000 modules		9400 modules
92 Mega-pixels		1.4 Giga-pixels

Planar Sensors

Layers L0-4 equipped with planar sensors:

- Outer layer (L1): 100 μm thickness
- Outer barrel and endcap (L2-4): 150 μm thickness
- Pixel size of 50x50 μm^2
- L2-4 expected to survive full amount of irradiation corresponding to 4000 fb^{-1}
- L1 replaced once ($\rightarrow$ 2000 fb^{-1})

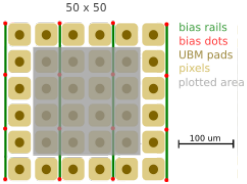

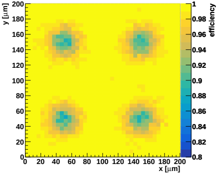

Testing Campaign:

- Visual inspection
- Electrical measurements
- Beam tests

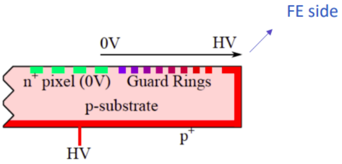

Planar Sensors

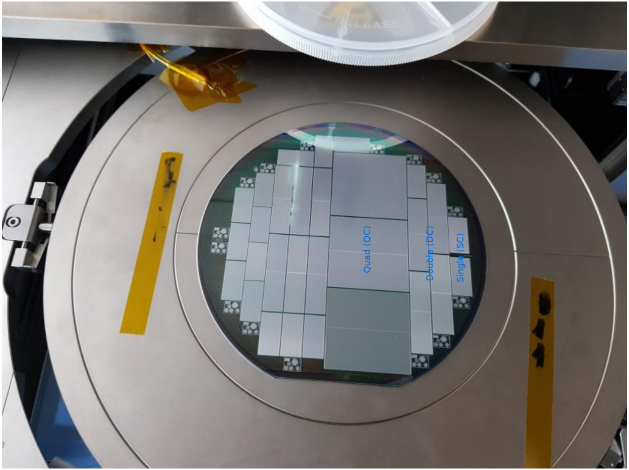

Single (SC), Double (DC), and Quad (QC) layouts

- Prototypes from various different foundries tested
- Final modules will all be quads

Visual Inspection

Visual inspection requirements:

- No stains, residues, scratches
- No chips $> 40\ \mu$m at edges
- No shorts between pixels
- Thickness and planarity requirements

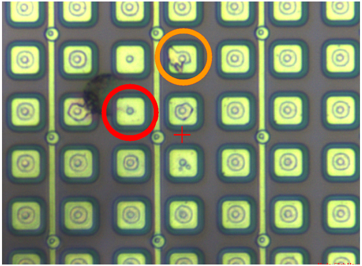

Results:

- Most sensors show no visual defects, some exceptions

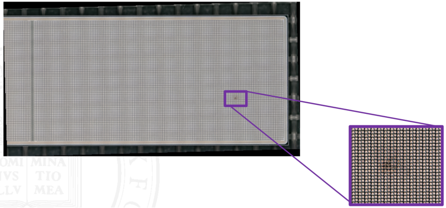

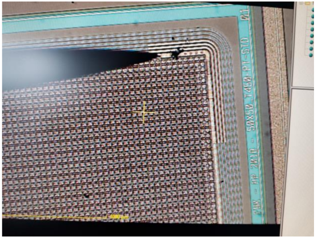

Electrical Characterization

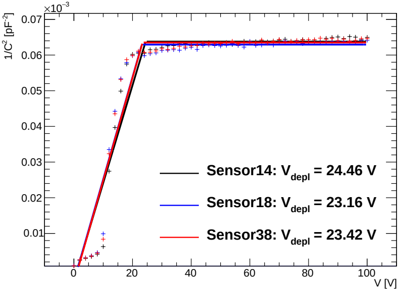

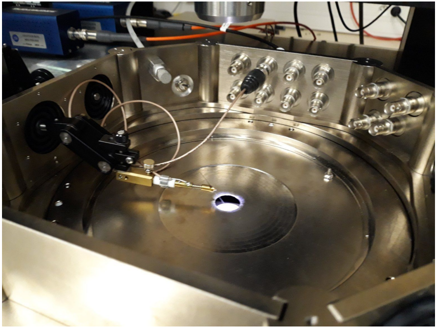

Requirements for Qualification:

- Depletion voltage $V_{dep} < 100$ V (for 150 μm sensors) measured at 1 kHz
- Leakage current $I_{leak} < 0.75\ \mu A/cm^2$ at $V_{dep} + 50$ V
- Variation of leakage current $\Delta I_{leak} < 25\%$ measured over 48 h
- Breakdown voltage $V_{break} > V_{dep} + 70$ V
  (V_{break} defined as V at which I_{leak} increases by $> 20\%$ over $\Delta V = 5$ V step)

Beam Tests

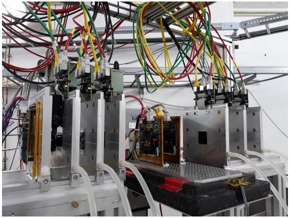

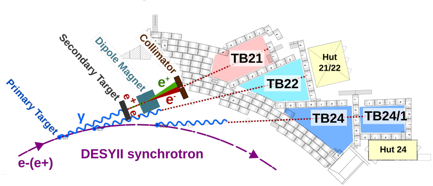

Hit effiecincy measurements at DESY test beam facility:

- Modules: Planar sensor bump-bonded to RD53 front end chip
- Unirradiated and irradiated to two fluences
- 3 measurement campaigns at DESY: Sep and Nov 2019, Jun 2020
- At least one measurement per vendor per fluence per thickness

Requirements on sensor efficiency:

	Measurement voltage	Fluence	Hit Efficiency
100 and 150 um thickness	Vdepl+50V	Before irradiation	>98.5%
100 um thickness	300V 400V	F=2x10^{15} n$_{eq}$/cm^{2}. F=5x10^{15} n$_{eq}$/cm^{2},	>97%
150 um thickness	400V 600V	F=2x10^{15} n$_{eq}$/cm^{2}, F=5x10^{15} n$_{eq}$/cm^{2},	>97%

Summary

Planar Pixel Sensors for the ATLAS ITk

ATLAS Inner Detector will be replaced with full-Si ITk:

- 1188 3D sensors at high-radiation inner layer
  - Pre-production started
  - 50×50 μm and 25×100 μm layout
- 8016 planar sensors in outer layers
  - 50×50 μm layout
  - Extensive Market Survey to qualify vendors
- Production for both sensor types forseen for mid 2022 - mid 2024
- QA/QC ongoing during pre-production and production
- Both type of sensors demonstrated necessary requirement for ITk

Additional Material

VBS/VBF at ATLAS

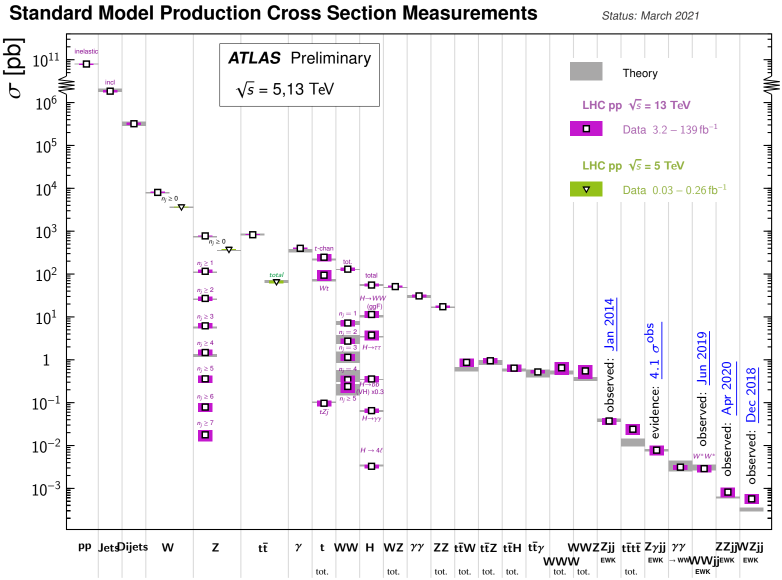

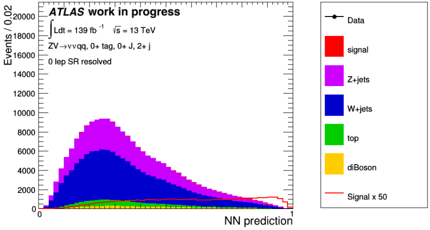

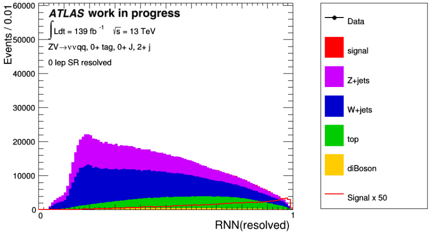

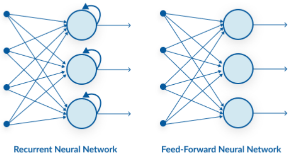

Baseline selection MVA:

- Simple feed-forward NN
- Using high-level input variables
- Tag-jet selection for VBS-like events
- But some VBS-like events lost by this

No-tag selection RNN:

- Dropping selection on j^{tag}
- Full jet four-vectors as inputs
  in addition to high level variables
- Recurrent architecture (RNN) allows variable input length
  Here: Each event has a different number of jets
- Rely on RNN to learn VBS-specific jet configuration

Fiducial Selection:

Object definition:

- ℓ^{good}: μ/e^{truth} with $p_T > 20$ GeV and $|\eta| < 2.5$
- ℓ^{veto}: μ/e^{truth} with $p_T > 7$ GeV and $|\eta| < 2.5$
- R=.4 jets j: j^{truth} with ($p_T > 20$ GeV and $|\eta| < 2.5$) or ($p_T > 30$ GeV and $|\eta| < 4.5$) and $\Delta R(\ell^{\text{good}}) > 0.2$
- R=1. jets J: J^{truth} with $p_T > 200$ GeV and $|\eta| < 2$
- b-labeled jet j_b: j with 'HadronConeExclTruthLabelID' = 5
- tag jets: highest-mass (jj) system from all j with $eta(j_1) * eta(j_2) < 0$ and not b-labeled
- resolved sig jets $(jj)^{\text{sig}}$: two leading p_T j excluding jj^{tag}
- merged sig jet J^{sig}: leading-p_T J with $\Delta R(j^{\text{tag}}) > 1.4$

Channel selections:

- 0-lepton:
  - $\not{E}_T > 200$ GeV
  - $== 0$ ℓ^{veto}
  - 0 or 2 b-tagged j^{sig}, no other
- 1-lepton:
  - $\not{E}_T > 80$ GeV
  - $== 1$ ℓ^{good}
  - $p_T(\ell^{\text{good}}) > 27$ GeV
  - no b-labeled jets
- 2-lepton:
  - $== 2$ ℓ^{good}
  - $p_T(\ell^{\text{good}}_{\text{lead}}) > 28$ GeV
  - $p_T(\ell^{\text{good}}_{\text{sub-lead}}) > 20$ GeV
  - 0 or 2 b-labeled j^{sig}, no other

Regime Definitions:

- merged: J^{sig} has $64 < m < 106$ GeV
- resolved: $(jj)^{\text{sig}}$ has $64 < m < 106$ GeV and $p_T(j^{\text{sig}}_{\text{lead}}) > 40$ GeV

Selection order (VBSFidType):

VBSFidType	channel	regime
0	0-lepton	merged
1	0-lepton	resolved
2	1-lepton	merged
3	1-lepton	resolved
4	2-lepton	merged
5	2-lepton	resolved

Tag jet selection (passFidMjjTag):

- p_T of both $j^{\text{tag}} > 30$ GeV
- $m(jj)^{\text{tag}} > 400$ GeV

Number of signal events after various extra selections to reduce non-VBS signal:

baseline selection:

	merged HP SR				merged LP SR				resolved SR			
selection	events	% fid.	% t	% V	events	% fid.	% t	% V	events	% fid.	% t	% V
nominal	68	43	10	4	114	40	12	5	1339	23	28	5
nominal+topMass	58	46	7	4	94	45	8	4	717	31	14	4
nominal+bVetoExcl	62	46	6	4	103	44	8	5	1197	25	22	5
nominal+bVetoExcl+topMass	55	48	5	3	88	47	6	4	683	32	12	4
nominal+bVetoExcl+bVetoSig	56	48	4	4	92	46	5	5	972	29	13	6
nominal+bVetoExcl+bVetoSig+topMass	50	50	4	4	80	49	4	4	588	35	7	5

no-tag selection:

	merged HP SR				merged LP SR				resolved SR			
selection	events	% fid.	% t	% V	events	% fid.	% t	% V	events	% fid.	% t	% V
nominal	130	23	25	15	233	20	28	15	2809	11	43	12
nominal+topMass	100	28	17	13	167	26	19	13	1253	19	27	10
nominal+bVetoExcl	105	28	14	16	185	25	16	16	2197	14	32	23
nominal+bVetoExcl+topMass	86	32	10	13	144	30	12	14	1096	21	31	10
nominal+bVetoExcl+bVetoSig	92	30	10	16	159	27	11	17	1680	17	20	15
nominal+bVetoExcl+bVetoSig+topMass	77	34	7	13	125	32	8	14	894	24	13	11

Extra cuts:

- **topMass:** $m_t > 200$ GeV where m_t: mass of $(jj)^{sig}$ + additional jet (triplet closest to SM top mass)
- **bVetoExcl:** no R= .4 jet (excl. sig jets) b-tagged
- **bVetoSig:** $==$ 0 or 2 signal jets b-tagged

Fractions:

- % **fid:** Fraction of events passing fiducial selection (resolved + merged combined)
- % **t:** Fraction of events that have a top in the diagram (truth info)

Reweighting

$m(jj)^{\text{tag}}$ reweighting in 0-lepton:

- Well-known mismodeling in Sherpa W/Z+jets samples
- Common issue among VBS/VBF analyses
- $m(jj)^{\text{tag}}$ reweighting derived in 1-lepton/2-lepton (W/Z) CR too strong for 0-lepton
- Independently deriving W and Z reweightings in 0-lepton CR reduces slope substantially

Procedure:

Fit ratio of W/Z+jets to data - all other MC

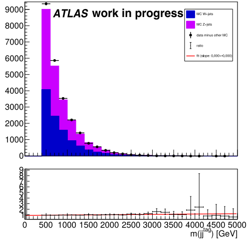

no reweighting

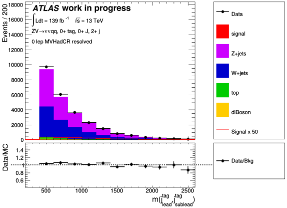

negative slope

reweighting from 1/2-lep

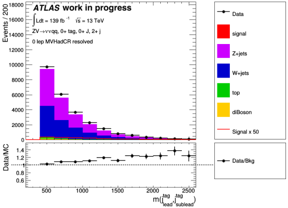

positive slope

reweighting from 0-lep

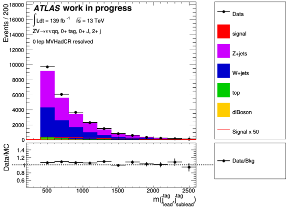

constant

Shape systematics (0-lepton):

- Shape systs. from ratio of shape in Sherpa (nominal) and MadGraph (syst)
- Normalized to MadGraph
- Rebinned (from right to left: merge bins with $<$ 50 events)
- Two options: With and without $m(jj)$ reweighting in Sherpa

W+jets:

merged HP SR

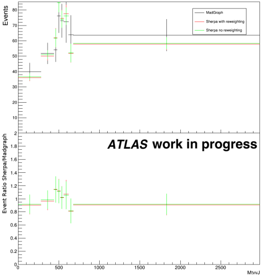

merged LP SR

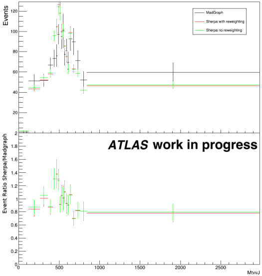

resolved SR

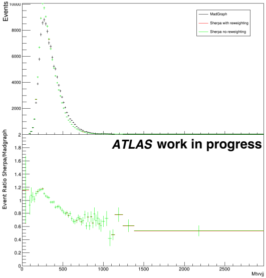

Shape systematics (0-lepton):
Z+jets:

merged HP SR

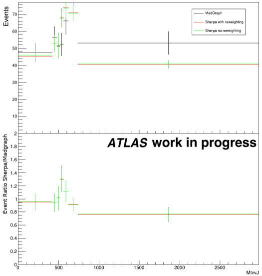

merged LP SR

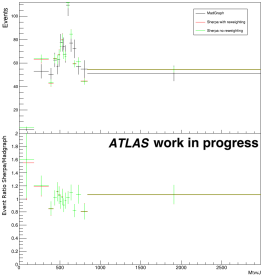

resolved SR

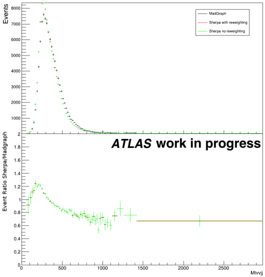

0lep Cut Flow

merged HP SR

cut	all MC	signal	background	s/b
All	15242638.1	10184.6	15232453.5	0.001
E_T^{miss} Trigger	15242638.1	10184.6	15232453.5	0.001
$N(j^{tag}) \geq 2$	9347195.5	7421.3	9339774.2	0.001
$p_T(j^{tag}_{lead}) > 30$ GeV	9295480.3	7400.0	9288080.3	0.001
$p_T(j^{tag}_{sublead}) > 30$ GeV	6718390.2	6357.9	6712032.3	0.001
$E_T^{miss} > 200$ GeV	2270267.2	2983.8	2267283.4	0.001
$E_T^{miss,track} > 50$ GeV	2064763.9	2674.7	2062089.2	0.001
$\lvert\Delta\Phi(E_T^{miss}, E_T^{miss,track})\rvert/\pi < \frac{1}{2}$	2018550.4	2566.0	2015984.4	0.001
$\min\{\lvert\Delta\Phi(E_T^{miss}, j_i^{smallR})\rvert\}_i/\pi < \frac{1}{6}$	1286141.7	1521.0	1284620.8	0.001
$N(J) \geq 1$	118538.2	284.9	118253.3	0.002
$\lvert\Delta\Phi(E_T^{miss}, J)\rvert/\pi < \frac{1}{9}$	115133.3	274.1	114859.2	0.002
$p_T(J) > 200$ GeV	115133.3	274.1	114859.2	0.002
$\lvert\eta(J)\rvert > 2.0$	115133.3	274.1	114859.2	0.002
$m(J) > 50$ GeV	49445.2	195.7	49249.5	0.004
D2FatJet2Var	21561.4	123.3	21438.1	0.006
TaggerFatJet2Var	5377.2	71.6	5305.7	0.013
$N(j^b) = 0$	3075.0	54.9	3020.1	0.018
$m(jj)^{tag} > 400$ GeV	2407.4	52.2	2355.2	0.022

→ merged LP SR

cut	all MC	signal	background	s/b
All	15240230.6	10132.3	15230098.3	0.001
E_T^{miss} Trigger	15240230.6	10132.3	15230098.3	0.001
$N(j^{tag}) \geq 2$	9344788.1	7369.1	9337419.0	0.001
$p_T(j^{tag}_{lead}) > 30$ GeV	9293072.9	7347.8	9285725.1	0.001
$p_T(j^{tag}_{sublead}) > 30$ GeV	6715982.8	6305.7	6709677.1	0.001
$E_T^{miss} > 200$ GeV	2267859.8	2931.6	2264928.2	0.001
$E_T^{miss,track} > 50$ GeV	2062356.5	2622.5	2059734.0	0.001
$\lvert\Delta\Phi(E_T^{miss}, E_T^{miss,track})\rvert/\pi < \frac{1}{2}$	2016142.9	2513.7	2013629.2	0.001
$\min\{\lvert\Delta\Phi(E_T^{miss}, j_i^{smallR})\rvert\}_i/\pi < \frac{1}{6}$	1283734.3	1468.7	1282265.6	0.001
$N(J) \geq 1$	116130.8	232.7	115898.1	0.002
$\lvert\Delta\Phi(E_T^{miss}, J)\rvert/\pi < \frac{1}{9}$	112725.8	221.9	112504.0	0.002
$p_T(J) > 200$ GeV	112725.8	221.9	112504.0	0.002
$m(J) > 50$ GeV	47037.7	143.4	46894.3	0.003
D2FatJet3Var	34852.1	114.5	34737.6	0.003
TaggerFatJet3Var	13743.9	69.8	13674.2	0.005
$N(j^b) = 0$	7842.3	39.1	7803.2	0.005
$m(jj)^{tag} > 400$ GeV	5783.7	34.2	5749.5	0.006

→ resolved SR

cut	all MC	signal	background	s/b
All	15234446.9	10098.1	15224348.8	0.001
E_T^{miss} Trigger	15234446.9	10098.1	15224348.8	0.001
$N(j^{tag}) \geq 2$	9339004.4	7334.9	9331669.5	0.001
$p_T(j^{tag}_{lead}) > 30$ GeV	9287289.2	7313.6	9279975.6	0.001
$p_T(j^{tag}_{sublead}) > 30$ GeV	6710199.0	6271.5	6703927.5	0.001
$E_T^{miss} > 200$ GeV	2262076.0	2897.4	2259178.6	0.001
$E_T^{miss,track} > 50$ GeV	2056572.8	2588.3	2053984.5	0.001
$\lvert\Delta\Phi(E_T^{miss}, E_T^{miss,track})\rvert/\pi < \frac{1}{2}$	2010359.2	2479.6	2007879.7	0.001
$\min\{\lvert\Delta\Phi(E_T^{miss}, j_i^{smallR})\rvert\}_i/\pi < \frac{1}{6}$	1277950.6	1434.5	1276516.0	0.001
$\lvert\Delta\Phi(E_T^{miss}, jj)\rvert/\pi < \frac{1}{9}$	1203645.3	1386.4	1202258.9	0.001
$N(j^{sig}) \geq 2$	723072.8	1167.2	721905.7	0.002
$p_T(j^{sig}_{lead}) > 40$ GeV	568652.1	1069.0	567583.1	0.002
$p_T(j^{sig}_{sublead}) > 20$ GeV	568652.1	1069.0	567583.1	0.002
$m(jj)^{sig} > 50$ GeV	518234.0	1020.8	517213.2	0.002
$N(j^b) = 0$	387375.8	639.9	386735.9	0.002
$m(jj)^{tag} > 400$ GeV	262707.3	531.4	262175.9	0.002

→ merged HP CR

cut	all MC	signal	background	s/b
All	14971739.6	9566.7	14962172.9	0.001
E_T^{miss} Trigger	14971739.6	9566.7	14962172.9	0.001
$N(j^{tag}) \geq 2$	9076297.1	6803.5	9069493.6	0.001
$p_T(j^{tag}_{lead}) > 30$ GeV	9024581.9	6782.2	9017799.6	0.001
$p_T(j^{tag}_{sublead}) > 30$ GeV	6447491.7	5740.1	6441751.6	0.001
$E_T^{miss} > 200$ GeV	1999368.7	2366.0	1997002.7	0.001
$E_T^{miss,track} > 50$ GeV	1793865.5	2056.9	1791808.6	0.001
$\lvert\Delta\Phi(E_T^{miss}, E_T^{miss,track})\rvert/\pi < \frac{1}{2}$	1747651.9	1948.1	1745703.8	0.001
$\min\{\lvert\Delta\Phi(E_T^{miss}, j_i^{smallR})\rvert\}_i/\pi < \frac{1}{6}$	1015243.3	903.1	1014340.1	0.001
$\lvert\Delta\Phi(E_T^{miss}, J)\rvert/\pi < \frac{1}{9}$	907416.9	810.0	906607.0	0.001
$N(J) \geq 1$	62179.0	110.4	62068.7	0.002
$p_T(J) > 200$ GeV	62179.0	110.4	62068.7	0.002
$\lvert\eta(J)\rvert > 2.0$	62179.0	110.4	62068.7	0.002
$m(J) > 50$ GeV	24913.7	72.2	24841.6	0.003
D2FatJet2Var	11460.4	43.5	11416.9	0.004
NotMassFatJet2Var	6324.8	17.7	6307.1	0.003
$N(j^b) = 0$	1658.6	2.5	1656.1	0.002
$m(jj)^{tag} > 400$ GeV	543.1	1.2	541.9	0.002

→ merged LP CR

cut	all MC	signal	background	s/b
All	14971196.5	9565.6	14961630.9	0.001
E_T^{miss} Trigger	14971196.5	9565.6	14961630.9	0.001
$N(j^{tag}) \geq 2$	9075754.0	6802.3	9068951.6	0.001
$p_T(j^{tag}_{lead}) > 30$ GeV	9024038.8	6781.0	9017257.7	0.001
$p_T(j^{tag}_{sublead}) > 30$ GeV	6446948.6	5738.9	6441209.7	0.001
$E_T^{miss} > 200$ GeV	1998825.6	2364.8	1996460.8	0.001
$E_T^{miss,track} > 50$ GeV	1793322.4	2055.7	1791266.6	0.001
$\lvert\Delta\Phi(E_T^{miss}, E_T^{miss,track})\rvert/\pi < \frac{1}{2}$	1747108.8	1947.0	1745161.8	0.001
$\min\{\lvert\Delta\Phi(E_T^{miss}, j_i^{smallR})\rvert\}_i/\pi < \frac{1}{6}$	1014700.2	902.0	1013798.2	0.001
$\lvert\Delta\Phi(E_T^{miss}, J)\rvert/\pi < \frac{1}{9}$	906873.8	808.8	906065.0	0.001
$N(J) \geq 1$	61635.9	109.2	61526.8	0.002
$p_T(J) > 200$ GeV	61635.9	109.2	61526.8	0.002
$m(J) > 50$ GeV	24370.6	71.0	24299.6	0.003
D2FatJet3Var	18448.0	59.1	18388.9	0.003
NotMassFatJet3Var	7817.8	19.3	7798.5	0.002
$N(j^b) = 0$	1907.9	2.0	1905.9	0.001
$m(jj)^{tag} > 400$ GeV	442.4	0.7	441.7	0.002

→ resolved CR

cut	all MC	signal	background	s/b
All	14970754.1	9564.9	14961189.3	0.001
E_T^{miss} Trigger	14970754.1	9564.9	14961189.3	0.001
$N(j^{tag}) \geq 2$	9075311.6	6801.6	9068510.0	0.001
$p_T(j^{tag}_{lead}) > 30$ GeV	9023596.4	6780.3	9016816.1	0.001
$p_T(j^{tag}_{sublead}) > 30$ GeV	6446506.3	5738.2	6440768.0	0.001
$E_T^{miss} > 200$ GeV	1998383.2	2364.1	1996019.1	0.001
$E_T^{miss,track} > 50$ GeV	1792880.0	2055.0	1790825.0	0.001
$\lvert\Delta\Phi(E_T^{miss}, E_T^{miss,track})\rvert/\pi < \frac{1}{2}$	1746666.4	1946.3	1744720.2	0.001
$\min\{\lvert\Delta\Phi(E_T^{miss}, j_i^{smallR})\rvert\}_i/\pi < \frac{1}{6}$	1014257.8	901.3	1013356.5	0.001
$\lvert\Delta\Phi(E_T^{miss}, jj)\rvert/\pi < \frac{1}{9}$	940082.4	853.4	939229.1	0.001
$N(j^{sig}) \geq 2$	459712.2	634.9	459077.3	0.001
$p_T(j^{sig}_{lead}) > 40$ GeV	305841.8	537.3	305304.5	0.002
$p_T(j^{sig}_{sublead}) > 20$ GeV	305841.8	537.3	305304.5	0.002
NotMVHadRes	139116.1	198.1	138918.1	0.001
$N(j^b) = 0$	93122.3	69.3	93053.0	0.001
$m(jj)^{tag} > 400$ GeV	24977.0	27.0	24950.0	0.001

Table: Sequential event yields scaled to a luminosity of 139 fb^{-1} in all signal (SR) and control (CR) regions after each consecutive cut.

0lep Cut Flow Raw

merged HP SR →

cut	all MC	signal	background	s/b
All	130068341.0	1614919.0	128453422.0	0.013
$E_{\mathrm{T}}^{\mathrm{miss}}$ Trigger	130068341.0	1614919.0	128453422.0	0.013
$\mathrm{N}(j^{\mathrm{tag}}) \geq 2$	80276923.0	1286189.0	78990734.0	0.016
$p_{\mathrm{T}}(j^{\mathrm{tag}}_{\mathrm{lead}}) > 30$ GeV	79845180.0	1284639.0	78560541.0	0.016
$p_{\mathrm{T}}(j^{\mathrm{tag}}_{\mathrm{sublead}}) > 30$ GeV	60927736.0	1162385.0	59765351.0	0.019
$E_{\mathrm{T}}^{\mathrm{miss}} > 200$ GeV	28976201.0	615826.0	28360375.0	0.022
$E_{\mathrm{T}}^{\mathrm{miss,track}} > 50$ GeV	26535379.0	557148.0	25978231.0	0.021
$\vert\Delta\Phi(E_{\mathrm{T}}^{\mathrm{miss}}, E_{\mathrm{T}}^{\mathrm{miss,track}})\vert/\pi < \frac{1}{2}$	25111540.0	537173.0	24574367.0	0.022
$\min\{\vert\Delta\Phi(E_{\mathrm{T}}^{\mathrm{miss}}, j_i^{\mathrm{smallR}})\vert\}_i/\pi < \frac{1}{6}$	14498184.0	347047.0	14151137.0	0.025
$\mathrm{N}(J) \geq 1$	2098048.0	69004.0	2029044.0	0.034
$\vert\Delta\Phi(E_{\mathrm{T}}^{\mathrm{miss}}, J)\vert/\pi < \frac{1}{9}$	2020023.0	68251.0	1951772.0	0.035
$p_{\mathrm{T}}(J) > 200$ GeV	2020023.0	68251.0	1951772.0	0.035
$\vert\eta(J)\vert > 2.0$	2020023.0	68251.0	1951772.0	0.035
$m(J) > 50$ GeV	903169.0	48607.0	854562.0	0.057
D2FatJet2Var	413011.0	31141.0	381870.0	0.082
TaggerFatJet2Var	80322.0	19332.0	60990.0	0.317
$\mathrm{N}(j^{b}) = 0$	53350.0	15219.0	38131.0	0.399
$m(jj)^{\mathrm{tag}} > 400$ GeV	46817.0	14591.0	32226.0	0.453

merged LP SR →

cut	all MC	signal	background	s/b
All	130021524.0	1600328.0	128421196.0	0.012
$E_{\mathrm{T}}^{\mathrm{miss}}$ Trigger	130021524.0	1600328.0	128421196.0	0.012
$\mathrm{N}(j^{\mathrm{tag}}) \geq 2$	80230106.0	1271598.0	78958508.0	0.016
$p_{\mathrm{T}}(j^{\mathrm{tag}}_{\mathrm{lead}}) > 30$ GeV	79798363.0	1270048.0	78528315.0	0.016
$p_{\mathrm{T}}(j^{\mathrm{tag}}_{\mathrm{sublead}}) > 30$ GeV	60880919.0	1147794.0	59733125.0	0.019
$E_{\mathrm{T}}^{\mathrm{miss}} > 200$ GeV	28929384.0	601235.0	28328149.0	0.021
$E_{\mathrm{T}}^{\mathrm{miss,track}} > 50$ GeV	26488562.0	542557.0	25946005.0	0.021
$\vert\Delta\Phi(E_{\mathrm{T}}^{\mathrm{miss}}, E_{\mathrm{T}}^{\mathrm{miss,track}})\vert/\pi < \frac{1}{2}$	25064723.0	522582.0	24542141.0	0.021
$\min\{\vert\Delta\Phi(E_{\mathrm{T}}^{\mathrm{miss}}, j_i^{\mathrm{smallR}})\vert\}_i/\pi < \frac{1}{6}$	14451367.0	332456.0	14118911.0	0.024
$\mathrm{N}(J) \geq 1$	2051231.0	54413.0	1996818.0	0.027
$\vert\Delta\Phi(E_{\mathrm{T}}^{\mathrm{miss}}, J)\vert/\pi < \frac{1}{9}$	1973206.0	53660.0	1919546.0	0.028
$p_{\mathrm{T}}(J) > 200$ GeV	1973206.0	53660.0	1919546.0	0.028
$m(J) > 50$ GeV	856352.0	34016.0	822336.0	0.041
D2FatJet3Var	622245.0	26858.0	595387.0	0.045
TaggerFatJet3Var	188623.0	17566.0	171057.0	0.103
$\mathrm{N}(j^{b}) = 0$	115457.0	9936.0	105521.0	0.094
$m(jj)^{\mathrm{tag}} > 400$ GeV	95706.0	8855.0	86851.0	0.102

resolved SR

cut	all MC	signal	background	s/b
All	129925818.0	1591473.0	128334345.0	0.012
$E_{\mathrm{T}}^{\mathrm{miss}}$ Trigger	129925818.0	1591473.0	128334345.0	0.012
$\mathrm{N}(j^{\mathrm{tag}}) \geq 2$	80134400.0	1262743.0	78871657.0	0.016
$p_{\mathrm{T}}(j^{\mathrm{tag}}_{\mathrm{lead}}) > 30$ GeV	79702657.0	1261193.0	78441464.0	0.016
$p_{\mathrm{T}}(j^{\mathrm{tag}}_{\mathrm{sublead}}) > 30$ GeV	60785213.0	1138939.0	59646274.0	0.019
$E_{\mathrm{T}}^{\mathrm{miss}} > 200$ GeV	28833678.0	592380.0	28241298.0	0.021
$E_{\mathrm{T}}^{\mathrm{miss,track}} > 50$ GeV	26392856.0	533702.0	25859154.0	0.021
$\vert\Delta\Phi(E_{\mathrm{T}}^{\mathrm{miss}}, E_{\mathrm{T}}^{\mathrm{miss,track}})\vert/\pi < \frac{1}{2}$	24969017.0	513727.0	24455290.0	0.021
$\min\{\vert\Delta\Phi(E_{\mathrm{T}}^{\mathrm{miss}}, j_i^{\mathrm{smallR}})\vert\}_i/\pi < \frac{1}{6}$	14355661.0	323601.0	14032060.0	0.023
$\vert\Delta\Phi(E_{\mathrm{T}}^{\mathrm{miss}}, jj)\vert/\pi < \frac{1}{9}$	13546943.0	312941.0	13234002.0	0.024
$\mathrm{N}(j^{\mathrm{sig}}) \geq 2$	8477981.0	261208.0	8216773.0	0.032
$p_{\mathrm{T}}(j^{\mathrm{sig}}_{\mathrm{lead}}) > 40$ GeV	6847000.0	240436.0	6606564.0	0.036
$p_{\mathrm{T}}(j^{\mathrm{sig}}_{\mathrm{sublead}}) > 20$ GeV	6847000.0	240436.0	6606564.0	0.036
$m(jj)^{\mathrm{sig}} > 50$ GeV	6344314.0	229704.0	6114610.0	0.038
$\mathrm{N}(j^{b}) = 0$	4727812.0	160336.0	4567476.0	0.035
$m(jj)^{\mathrm{tag}} > 400$ GeV	3724357.0	136798.0	3587559.0	0.038

→ **merged HP CR**

cut	data	all MC	signal	background	s/b
All	39172871.0	126201461.0	1454675.0	124746786.0	0.012
$E_{\mathrm{T}}^{\mathrm{miss}}$ Trigger	39172871.0	126201461.0	1454675.0	124746786.0	0.012
$\mathrm{N}(j^{\mathrm{tag}}) \geq 2$	22186529.0	76410043.0	1125945.0	75284098.0	0.015
$p_{\mathrm{T}}(j^{\mathrm{tag}}_{\mathrm{lead}}) > 30$ GeV	22090335.0	75978300.0	1124395.0	74853905.0	0.015
$p_{\mathrm{T}}(j^{\mathrm{tag}}_{\mathrm{sublead}}) > 30$ GeV	16081162.0	57060856.0	1002141.0	56058715.0	0.018
$E_{\mathrm{T}}^{\mathrm{miss}} > 200$ GeV	3481122.0	25109321.0	455582.0	24653739.0	0.018
$E_{\mathrm{T}}^{\mathrm{miss,track}} > 50$ GeV	2713454.0	22668499.0	396904.0	22271595.0	0.018
$\vert\Delta\Phi(E_{\mathrm{T}}^{\mathrm{miss}}, E_{\mathrm{T}}^{\mathrm{miss,track}})\vert/\pi < \frac{1}{2}$	2509233.0	21244660.0	376929.0	20867731.0	0.018
$\min\{\vert\Delta\Phi(E_{\mathrm{T}}^{\mathrm{miss}}, j_i^{\mathrm{smallR}})\vert\}_i/\pi < \frac{1}{6}$	1043187.0	10631304.0	186803.0	10444501.0	0.018
$\vert\Delta\Phi(E_{\mathrm{T}}^{\mathrm{miss}}, J)\vert/\pi < \frac{1}{9}$	931883.0	9514583.0	168598.0	9345985.0	0.018
$\mathrm{N}(J) \geq 1$	59057.0	953164.0	25022.0	928142.0	0.027
$p_{\mathrm{T}}(J) > 200$ GeV	59057.0	953164.0	25022.0	928142.0	0.027
$\vert\eta(J)\vert > 2.0$	59057.0	953164.0	25022.0	928142.0	0.027
$m(J) > 50$ GeV	21271.0	376483.0	16006.0	360477.0	0.044
D2FatJet2Var	9762.0	170181.0	9479.0	160702.0	0.059
NotMassFatJet2Var	5418.0	105932.0	3065.0	102867.0	0.030
$\mathrm{N}(j^{b}) = 0$	1443.0	34302.0	579.0	33723.0	0.017
$m(jj)^{\mathrm{tag}} > 400$ GeV	448.0	17969.0	287.0	17682.0	0.016

→ **merged LP CR**

cut	data	all MC	signal	background	s/b
All	39172423.0	126183492.0	1454388.0	124729104.0	0.012
$E_{\mathrm{T}}^{\mathrm{miss}}$ Trigger	39172423.0	126183492.0	1454388.0	124729104.0	0.012
$\mathrm{N}(j^{\mathrm{tag}}) \geq 2$	22186081.0	76392074.0	1125658.0	75266416.0	0.015
$p_{\mathrm{T}}(j^{\mathrm{tag}}_{\mathrm{lead}}) > 30$ GeV	22089887.0	75960331.0	1124108.0	74836223.0	0.015
$p_{\mathrm{T}}(j^{\mathrm{tag}}_{\mathrm{sublead}}) > 30$ GeV	16080714.0	57042887.0	1001854.0	56041033.0	0.018
$E_{\mathrm{T}}^{\mathrm{miss}} > 200$ GeV	3480674.0	25091352.0	455295.0	24636057.0	0.018
$E_{\mathrm{T}}^{\mathrm{miss,track}} > 50$ GeV	2713006.0	22650530.0	396617.0	22253913.0	0.018
$\vert\Delta\Phi(E_{\mathrm{T}}^{\mathrm{miss}}, E_{\mathrm{T}}^{\mathrm{miss,track}})\vert/\pi < \frac{1}{2}$	2508785.0	21226691.0	376642.0	20850049.0	0.018
$\min\{\vert\Delta\Phi(E_{\mathrm{T}}^{\mathrm{miss}}, j_i^{\mathrm{smallR}})\vert\}_i/\pi < \frac{1}{6}$	1042739.0	10613335.0	186516.0	10426819.0	0.018
$\vert\Delta\Phi(E_{\mathrm{T}}^{\mathrm{miss}}, J)\vert/\pi < \frac{1}{9}$	931435.0	9496614.0	168311.0	9328303.0	0.018
$\mathrm{N}(J) \geq 1$	58609.0	935195.0	24735.0	910460.0	0.027
$p_{\mathrm{T}}(J) > 200$ GeV	58609.0	935195.0	24735.0	910460.0	0.027
$m(J) > 50$ GeV	20823.0	358514.0	15719.0	342795.0	0.046
D2FatJet3Var	15737.0	257907.0	12863.0	245044.0	0.052
NotMassFatJet3Var	6697.0	122487.0	3193.0	119294.0	0.027
$\mathrm{N}(j^{b}) = 0$	1632.0	31021.0	458.0	30563.0	0.015
$m(jj)^{\mathrm{tag}} > 400$ GeV	390.0	10193.0	167.0	10026.0	0.017

→ **resolved CR**

cut	data	all MC	signal	background	s/b
All	39172033.0	126173299.0	1454221.0	124719078.0	0.012
$E_{\mathrm{T}}^{\mathrm{miss}}$ Trigger	39172033.0	126173299.0	1454221.0	124719078.0	0.012
$\mathrm{N}(j^{\mathrm{tag}}) \geq 2$	22185691.0	76381881.0	1125491.0	75256390.0	0.015
$p_{\mathrm{T}}(j^{\mathrm{tag}}_{\mathrm{lead}}) > 30$ GeV	22089497.0	75950138.0	1123941.0	74826197.0	0.015
$p_{\mathrm{T}}(j^{\mathrm{tag}}_{\mathrm{sublead}}) > 30$ GeV	16080324.0	57032694.0	1001687.0	56031007.0	0.018
$E_{\mathrm{T}}^{\mathrm{miss}} > 200$ GeV	3480284.0	25081159.0	455128.0	24626031.0	0.018
$E_{\mathrm{T}}^{\mathrm{miss,track}} > 50$ GeV	2712616.0	22640337.0	396450.0	22243887.0	0.018
$\vert\Delta\Phi(E_{\mathrm{T}}^{\mathrm{miss}}, E_{\mathrm{T}}^{\mathrm{miss,track}})\vert/\pi < \frac{1}{2}$	2508395.0	21216498.0	376475.0	20840023.0	0.018
$\min\{\vert\Delta\Phi(E_{\mathrm{T}}^{\mathrm{miss}}, j_i^{\mathrm{smallR}})\vert\}_i/\pi < \frac{1}{6}$	1042349.0	10603142.0	186349.0	10416793.0	0.018
$\vert\Delta\Phi(E_{\mathrm{T}}^{\mathrm{miss}}, jj)\vert/\pi < \frac{1}{9}$	964244.0	9797930.0	175751.0	9622179.0	0.018
$\mathrm{N}(j^{\mathrm{sig}}) \geq 2$	424495.0	4734125.0	124230.0	4609895.0	0.027
$p_{\mathrm{T}}(j^{\mathrm{sig}}_{\mathrm{lead}}) > 40$ GeV	289998.0	3119068.0	103584.0	3015484.0	0.034
$p_{\mathrm{T}}(j^{\mathrm{sig}}_{\mathrm{sublead}}) > 20$ GeV	289998.0	3119068.0	103584.0	3015484.0	0.034
NotMVHadRes	138575.0	1451866.0	38434.0	1413432.0	0.027
$\mathrm{N}(j^{b}) = 0$	93943.0	822297.0	16094.0	806203.0	0.020
$m(jj)^{\mathrm{tag}} > 400$ GeV	24728.0	290406.0	6676.0	283730.0	0.024

Table: Non-scaled sequential event yields in all signal (SR) and control (CR) regions after each consecutive cut.

Analysis regions:

Regions		Discriminants		
		Merged high-purity	Merged low-purity	Resolved
0-lepton	SR	BDT	BDT	BDT
	VjjCR	m_{jj}^{tag}	m_{jj}^{tag}	m_{jj}^{tag}
1-lepton	SR	BDT	BDT	BDT
	WCR	m_{jj}^{tag}	m_{jj}^{tag}	m_{jj}^{tag}
	TopCR	One bin	One bin	One bin
2-lepton	SR	BDT	BDT	BDT
	ZCR	m_{jj}^{tag}	m_{jj}^{tag}	m_{jj}^{tag}

Baseline MVA inputs:

merged:

Variable	0-lepton	1-lepton	2-lepton
m_{jj}^{tag}	✓	–	✓
$\Delta\eta_{jj}^{\text{tag}}$	–	–	✓
$p_{\text{T}}^{\text{tag},j_2}$	✓	✓	✓
m_J	✓	–	–
$D_2^{(\beta=1)}$	✓	–	✓
$E_{\text{T}}^{\text{miss}}$	✓	–	–
$\Delta\phi(\vec{E}_{\text{T}}^{\text{miss}}, J)$	✓	–	–
η_ℓ	–	✓	–
$n_{j,\text{track}}$	✓	–	–
ζ_V	–	✓	✓
m_{VV}	–	–	✓
p_{T}^{VV}	–	–	✓
m_{VVjj}	–	✓	–
p_{T}^{VVjj}	–	–	✓
w^{tag,j_1}	✓	–	–
w^{tag,j_2}	✓	–	–

resolved:

Variable	0-lepton	1-lepton	2-lepton
m_{jj}^{tag}	✓	–	✓
$\Delta\eta_{jj}^{\text{tag}}$	–	–	✓
$p_{\text{T}}^{\text{tag},j_1}$	✓	✓	–
$p_{\text{T}}^{\text{tag},j_2}$	✓	✓	✓
$\Delta\eta_{jj}$	✓	✓	✓
$p_{\text{T}}^{j_1}$	✓	–	–
$p_{\text{T}}^{j_2}$	✓	✓	✓
w^{j_1}	✓	✓	✓
w^{j_2}	✓	✓	✓
$n_{\text{tracks}}^{j_1}$	–	✓	✓
$n_{\text{tracks}}^{j_2}$	–	✓	✓
w^{tag,j_1}	✓	✓	✓
w^{tag,j_2}	✓	✓	✓
$n_{\text{tracks}}^{\text{tag},j_1}$	–	✓	✓
$n_{\text{tracks}}^{\text{tag},j_2}$	–	✓	✓
$n_{j,\text{track}}$	✓	–	✓
$n_{j,\text{extr}}$	✓	–	–
$E_{\text{T}}^{\text{miss}}$	✓	–	–
η_ℓ	–	✓	–
$\Delta R(\ell, \nu)$	–	✓	–
ζ_V	–	✓	✓
m_{VV}	–	–	✓
m_{VVjj}	–	✓	–

Object Definition: Jets

Small-R-jets j:

- EMPFlow
- AntiKt with $R = 0.4$
- $p_{\mathrm{T}}(j) > 20$ GeV

Large-R-jets J:

- LCTopo
- AntiKt with $R = 1.0$
- $p_{\mathrm{T}}(J) > 200$ GeV
- Trimmed with $f_{\mathrm{cut}} = 5.0$, $R_{\mathrm{sub}} = 0.2$ (Kt-reclustering)

Track-jets $j^{\mathbf{track}}$:

- From PV0-Tracks
- AntiKt with $R = 0.2$

Tagging Jets $(jj)^{\mathbf{tag}}$:

- dijet small-R-jet system jj with:
- $\Delta\eta(jj) < 0$
- $\max(m_{jj})$

Signal jets $(jj)^{\mathbf{sig}}$:

- dijet small-R-jet system jj with:
- $\min(|m_{W/Z} - m_{jj}|)$
- selected after tagging jets

Signal fat jet $J^{\mathbf{sig}}$:

- leading p_{T} large-R-jet J
- with $\Delta R(J, j^{\mathrm{tag}}) > 1.4$

B-tagging:

- MV2c10 algorithm
- $\epsilon = 70\%$ working point (in $t\bar{t}$)

Object Reconstruction:

- e: isolated clusters in EMcal matched to ID tracks
  - $E_T > 7$ GeV
  - $|\eta| < 2.47$
  - {loose,medium,tight} id to separate from hadrons
- μ: combined fit from MS and ID
  - $p_T > 7$ GeV
  - $|\eta| < 2.5$
  - {loose,medium,tight} id from #hits in ID and $|\frac{q}{p_{MS}} - \frac{q}{p_{ID}}|$
- I(e,μ) isolation:
  - from $\sum p_T$ of tracks in p_T-dep. cone around I
- jets: EMPFlow(R=0.4)+LCTopo(R=1.0)
- b-tagging for j at 70% (in $t\bar{t}$), rejection factor: 380(L), 12(C)
- j(R=0.4):
  - $p_T > 20$ GeV at $|\eta| < 2.5$, $p_T > 30$ GeV at $2.5 < |\eta| < 4.5$
  - vertex tagger PU supr. for j with $p_T < 60$ GeV and $|\eta| < 2.5$
- J(R=1.0):
  - $p_T > 200$ GeV, $|\eta| < 2.0$
- j^{track}(R=0.2) (#j^{track} used as BDT input):
  - $p_T > 20$ GeV, $|\eta| < 2.5$
- E_T^{miss} : neg. vectorial sum of $p_T(e, \mu, j)$
- p_T^{miss} : neg. vectorial sum of all good ID tracks assoc. to PV

Overlap Removal:

- j removed if $\Delta R(j, e) < 0.2$
- e removed if $0.2 < \Delta R(j, e) < 0.4$
- j removed if $\Delta R(j, \mu) < 0.2$ and (j has < 3 tracks or small $\Delta E, p(j, \mu)$)
- μ removed if $0.2 < \Delta R(j, \mu) < 0.4$
- J removed if $\Delta R(J, e) < 1.0$
- no overlap removal between J, j, and j^{track}

W/Z tagging (in J):

- p_{T} dependent requirement on $D_2^{(\beta=1)}$
- must be in p_{T} dependent window around m_{boson}
- working points of 50% and 80%

2019-08-22: Previous Analysis with 35.5 fb^{-1}: Phys. Rev. D 100, 032007

Prev. Analyis: 0Lep Event yields:

Sample		Resolved	Merged HP	Merged LP
Background	W + jets	9200 ± 1300	259 ± 27	582 ± 56
	Z + jets	$19\,000 \pm 1400$	383 ± 29	955 ± 69
	Top quarks	3280 ± 480	277 ± 28	276 ± 32
	Diboson	720 ± 120	69 ± 12	68 ± 14
	Total	$32\,100 \pm 2000$	988 ± 50	1881 ± 96
Signal	$W(\ell\nu)W(qq')$	56 ± 22	8.0 ± 3.2	5.4 ± 2.2
	$W(\ell\nu)Z(qq)$	12.0 ± 4.7	2.1 ± 0.8	1.6 ± 0.6
	$Z(\nu\nu)W(qq')$	66 ± 25	9.0 ± 3.5	7.4 ± 2.9
	$Z(\nu\nu)Z(qq)$	27 ± 10	5.1 ± 2.0	3.1 ± 1.2
	Total	161 ± 35	24.3 ± 5.2	17.5 ± 3.9
SM		$32\,300 \pm 2000$	1012 ± 50	1898 ± 96
Data		32 299	1002	1935

Prev. Analysis: Uncertainties:

Uncertainty source	σ_μ
Total uncertainty	0.41
Statistical	0.20
Systematic	0.35
Theoretical and modeling uncertainties	
Floating normalizations	0.09
Z + jets	0.13
W+ jets	0.09
$t\bar{t}$	0.06
Diboson	0.09
Multijet	0.04
Signal	0.07
MC statistics	0.17
Experimental uncertainties	
Large-R jets	0.08
Small-R jets	0.06
Leptons	0.02
$E_{\mathrm{T}}^{\mathrm{miss}}$	0.04
b-tagging	0.07
Pileup	0.04
Luminosity	0.03

Electroweak Zjj (VBS):

- Leptonic decay: $\rightarrow \ell^+\ell^- jj$ $(\ell = e, \mu)$
- 8 TeV paper (20.3 fb^{-1}):
  5 σ observation
- First 13 TeV paper (3 fb^{-1}):
  Fiducial cross-section
- Current 13 TeV paper (139 fb^{-1}):

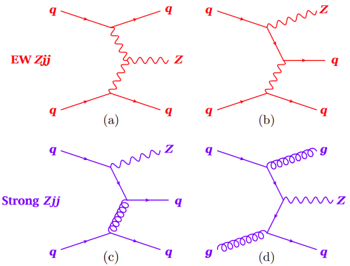

Differential x-sec measurement:

- With respect to 4 observables: $m(jj)$, $|\Delta y(jj)|$, $\Delta\Phi(jj)$, $p_T(\ell\ell)$
- Short term goal: Gives handle on which MC Generator models VBS/VBF most reliably
- Long term goal: Provides input for MC generator improvement

Search for anomalous weak-boson self-interactions:

- EFT approach
- Limits on 4 dim. 6 operators producing anomalous WWZ interactions

Electroweak ZZjj (VBS):

- 13 TeV paper (139 fb^{-1}):

  Final states: $\rightarrow \ell\ell\ell\ell jj$ and $\ell\ell\nu\nu jj$

  Combined: 5.5 σ

  One of the smallest cross-sections measured in ATLAS!

significance of EW Zjj:

	Significance Obs. (Exp.)
$\ell\ell\ell\ell jj$	5.5 (3.9) σ
$\ell\ell\nu\nu jj$	1.2 (1.8) σ
Combined	5.5 (4.3) σ

measured cross-section:

$$\sigma_{\text{EW}}^{\text{ZZjj}} = 0.82 \pm 0.21 \text{ fb}$$

EW production:

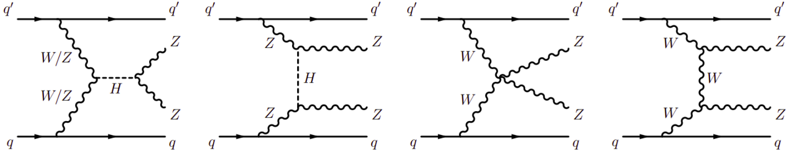

strong production:

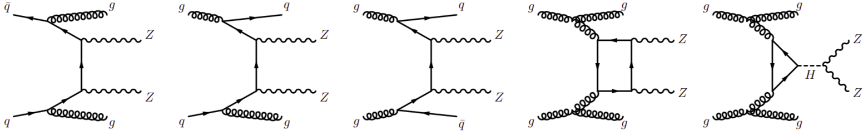

EW WWjj same sign (VBS):

- $W^{\pm}W^{\pm}jj$ has largest ratio of EW/QCD cross-section among VBS diboson
- Strong production not the dominant background
- 8 TeV paper (20.3 fb^{-1}):
  Evidence: 4.5 σ
- 13 TeV paper (36.1 fb^{-1}):
  observation: 6.5 σ
  fid. cross-section: $\sigma_{\text{EW}}^{W^{\pm}W^{\pm}jj} = 2.89$ fb

weak production:

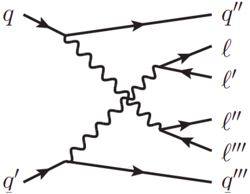

strong production:

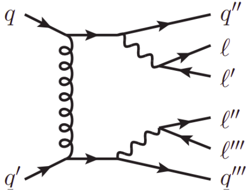

CR

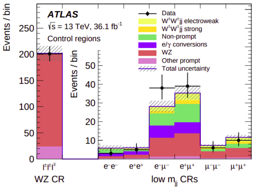

SR

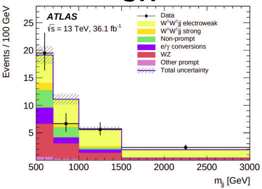

Non-prompt leptons bkg:

- ℓ from heavy-flavour hadrons
- Jets misidentified as e

- 6 channels: $e^{\pm}e^{\pm}$, $\mu^{\pm}\mu^{\pm}$, $e^{\pm}\mu^{\pm}$

$\Rightarrow$ 6 SRs ($\times$4 bins) + 6 m_{jj} CRs + WZ CR

ITk Requirements

Necessary properties:

- Radiation hardness
  - Up to $\approx 2 \times 10^{16}\ \frac{\text{neq}}{\text{cm}^2}$ (3D at L0)
  - Up to order of 10^7 Gy total ionizing doze (TID)
- Increased pileup
  - Up to 10 times more track density
  - Higher granularity
  - Higher burden on readout

Desired for physics:

- High spacial resolution
- High single-pixel hit efficiency

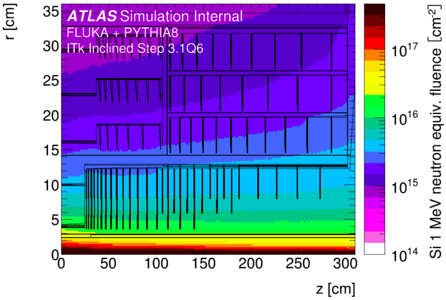

Planar sensor radiation requirements:

Layer	max. fluence n_{eq}/cm^2 (SF=1.5)	max. TID in MGy (SF=1.5)
L1 (@2000fb^{-1})	4.1e15	3,4
L2	4.7e15	5,2
L3	3.2e15	2,5
L4	2.4e15	1,4

Support

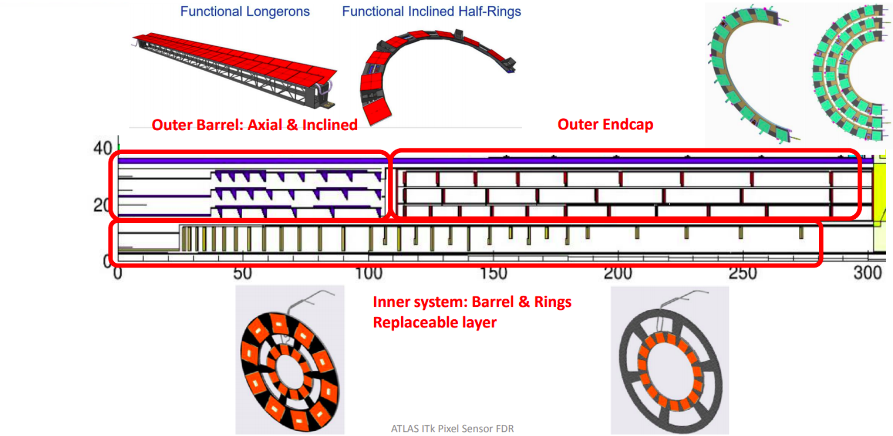
Functional Longerons
Functional Inclined Half-Rings
Outer Barrel: Axial & Inclined
Outer Endcap
40
20
0
0
50
100
150
200
250
300
Inner system: Barrel & Rings
Replaceable layer

Front End Chip

RDS53A prototype:

- Common R&D by ATLAS & CMS
- $50 \times 50\ \mu m$ grid
- Three analog FE

ITkPixV1/2 full size chip:

- Based on differential FE
- 1 MHz trigger rate
- Radiation hard up to > 5 MGy ($10^{16}\ \frac{neq}{cm^2}$)
- 65 nm technology
- First wafers of V1.1 available
- Final submission of V2 forseen before end of 2021

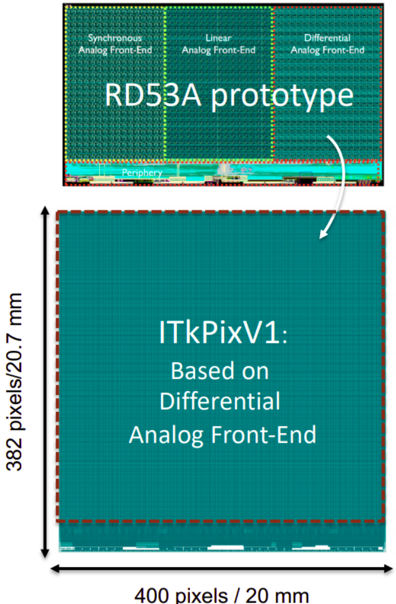

3D Sensors

Innermost layer L0 equipped with 3D sensors:

- Final design review (FDR) held 26 Nov 2019
- Proximity to beam requires superior radiation hardnes ($10^{16} \frac{\text{neq}}{\text{cm}^2}$)
- L0 replaceable after high irradiation damage
- Triplet module geometry
- Single-side technology (n&p electrodes etched from same side)
- 50×50 (rings) and 25x100 μm^2 (barrel) pixel size
- $> 97\%$ hit efficiency at 14° incl. ($> 96\%$ perpendicular)

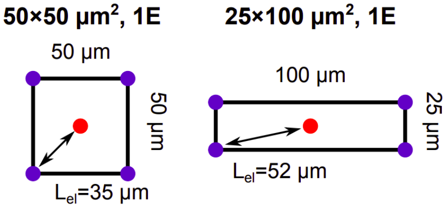

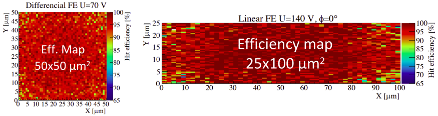

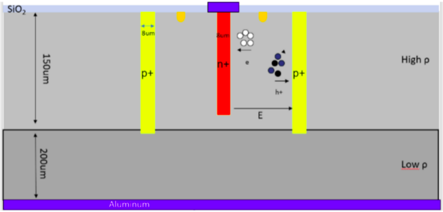

3D Sensors

- Low 80 – 140 V bias voltage
- Low power dissipation $< 10\ \frac{\text{mW}}{\text{cm}^2}$ ($@-25\ ^\circ\text{C},\ 10^{16}\frac{\text{neq}}{\text{cm}^2}$)
- More results for 3D sensors in 3D session on Thursday:
  - By Alessandro Lapertosa on FBK sensors
  - By Stefano Terzo on CNM sensors

Results for CNM sensors on RD53A:

power dissipation ($@10^{16}\frac{\text{neq}}{\text{cm}^2}$)

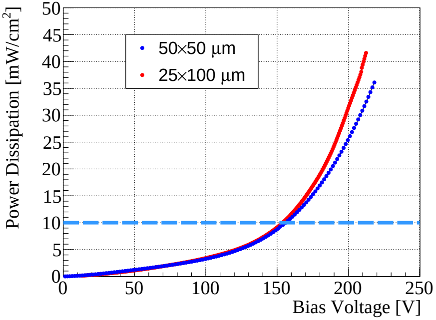

leakage current

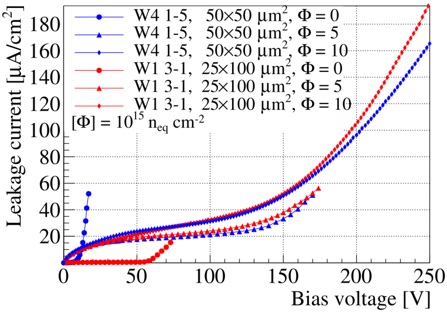

(Nuclear Instruments and Methods in Physics Research Section A, Vol 982)

Bias Structure

Bias structure allows check of leakage current before flip-chip:

- Several options from different vendors:
  - Poly-silicon bias resistor
    - Higher noise
  - Bias rail with punch-through (PT)
    - Reduced hit efficiency around PT dots
  - No bias structure
    - Needs temporary metal layer until wafer dicing
    - Uniform efficiency
    - No uniform ground in case of disconnected pixel

Poly-si bias resistor

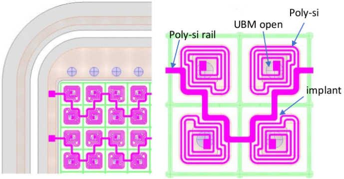

PT dot & bias rail

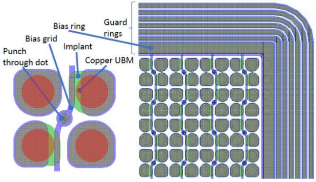

No bias structure

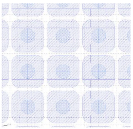

Koji Nakamura, ITk Week 2021-02-01

Thickness and Planarity

Some institutes have dedicated setup to perform laser scan

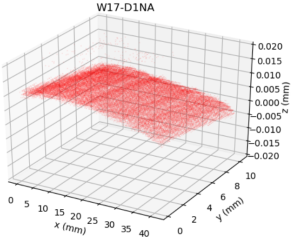

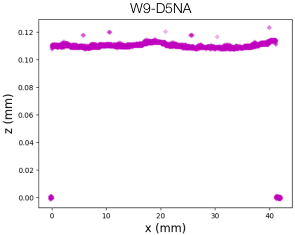

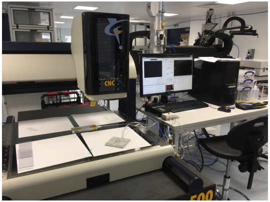

Other institutes: Microscope-focus method:

- Focus on several points on sensor and chuck by adjusting microscope height with fixed focal length
- Local thickness approximated as difference of height h between point on chuck and sensor

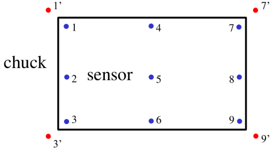

$$\text{thickness} = \langle h_i^{\text{sensor}} - h_i^{\text{chuck}} \rangle_{i\in[1,9]}$$

$$\text{planarity} = \frac{h_4 + h_5 + h_6}{3} - \frac{h_1 + h_2 + h_3 + h_7 + h_8 + h_9}{6}$$

CV and IV

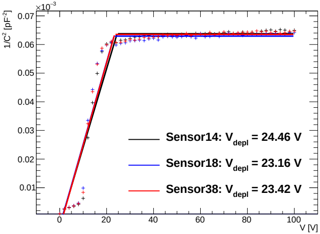

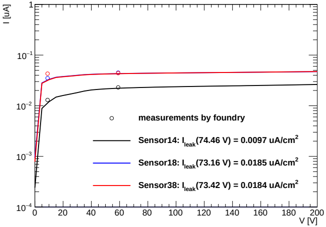

CV measurements:

- Plot $1/C^2$ vs V to calculate V_{dep}
- Perform 2 fits:
  - Constant in fully depleted region
  - Linear rise before
- V_{dep} given by the position of the intersection
- Requirement: $V_{\text{dep}} < 100V$ (for 150 μm)

IV measurements:

- Plot I vs V
- Increase by $\Delta I > 20\%$ over $\Delta V = 5V$ step defined as breakdown
- Requirement: $V_{\text{break}} > V_{\text{dep}} + 70$ V
- Requirement: $I_{\text{leak}}/\text{area} < 0.75\ \mu A/\text{cm}^2$ at $V_{\text{dep}} + 50$ V

CV and IV

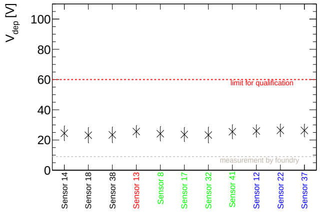

50x50 single 100x25 single 50x50 double 100x25 double

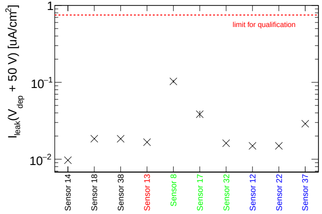

50x50 single 100x25 single 50x50 double 100x25 double

CV measurements:

- Plot $1/C^2$ vs V to calculate V_{dep}
- Perform 2 fits:
  - Constant in fully depleted region
  - Linear rise before
- V_{dep} given by the position of the intersection
- Requirement: $V_{dep} < 100V$ (for 150 μm)

IV measurements:

- Plot I vs V
- Increase by $\Delta I > 20\%$ over $\Delta V = 5V$ step defined as breakdown
- Requirement: $V_{break} > V_{dep} + 70$ V
- Requirement: $I_{leak}/\text{area} < 0.75\ \mu A/\text{cm}^2$ at $V_{dep} + 50$ V

Leakage Current Stability

It $(48\ \mathbf{h})\ V = V_{\mathbf{dep}} + 50\ \mathbf{V}$

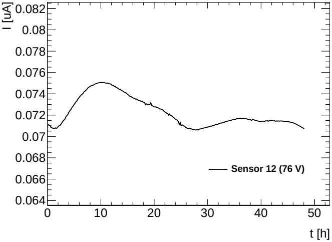

It measurements:

- Plot I at $V = V_{\text{dep}} + 50$ V
- Measure for 48 h
- Ensure stable humidity, temperature, and darkness
- Requirement: Variation $\Delta I_{\text{leak}} < 25\%$

ITk QA/QC

Quality Control (QC):

- Identify defects in finished sensors

Quality Assurance (QA):

- Prevent defects in production

	Production stage	Associated QA/QC
Pre-production	Sensor wafer production **(sensor vendor)**	- IV/CV - Visual inspection - Metrology
	After UBM - Thinning - Backside metallisation and dicing **(Hybridisation vendor)**	- IV - Metrology - Visual inspection
	On test structures and bare sensors at **ITk institutes**	- IV/CV/IT - Inter pixel R/C - Irradiations - CCE
	On flip-chipped modules at **ITk institutes**	- IV/IT - Irradiations - Test-beams
Production	Sensor wafer production **(sensor vendor)**	- IV/CV - Visual inspection - Metrology
	After UBM, Thinning, Backside metallisation and dicing **(Hybridisation vendor)**	- IV (?) - Metrology - Visual inspection
	On test structures at **ITk institutes**	- IV/CV/IT - Inter pixel R/C

ITk Schedule

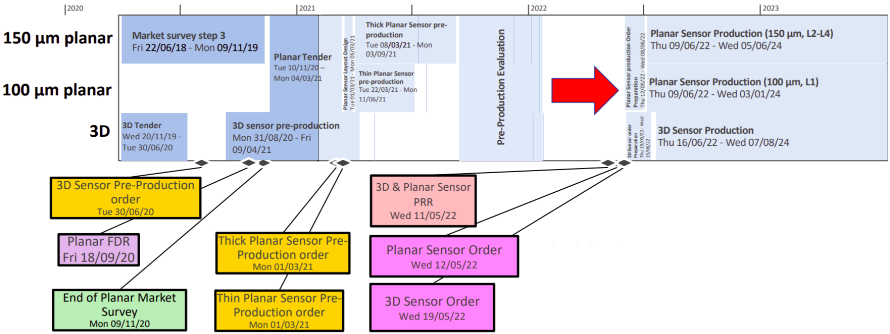

Planar sensors:

- Pre-prod.: Mar - Sep 2021
- Production: mid 2022 - mid 2024

3D sensors:

- Pre-prod.: Aug 2020 - Apr 2021
- Production: mid 2022 - mid 2024